Hindawi Publishing Corporation
International Journal of Optics
Volume 2013, Article ID 367967, 8 pages
http://dx.doi.org/10.1155/2013/367967

Research Article

Insight into PMD Regimes: An Analysis on Buried Optical Fibres

Winston T. Ireeta,[1,2] Vitalis Musara,[1] Lorinda Wu,[1] and Andrew W. R. Leitch[1]

[1] *Department of Physics, Makerere University, Kampala, Uganda*
[2] *Department of Physics, Optical Fibre Research Unit, P.O. Box 77000, Nelson Mandela Metropolitan University, Port Elizabeth 6031, South Africa*

Correspondence should be addressed to Winston T. Ireeta; ireeta@physics.mak.ac.ug

Received 9 January 2013; Revised 16 March 2013; Accepted 25 March 2013

Academic Editor: Ivan Djordjevic

Polarization mode dispersion (PMD) field measurements on deployed buried fibres showed that the PMD variation over the 1520 to 1570 nm wavelength was stochastic. The PMD variation over the 98-hour period for each wavelength was directional and limited; they are due to the presence of random mode coupling along the fibre length and limited influence from extrinsic perturbations over time, respectively. PMD variation in the wavelength domain showed that the mean first-order PMD (FO-PMD) value is independent of whether the FO-PMD statistics of a fibre link approaches the Maxwellian theoretical distribution; the key factor is sufficient random mode coupling. The accompanying second-order PMD (SO-PMD) statistics, with FO-PMD statistics approaching Maxwellian, followed the PDF given by Foschini et al. (1999). The FO- and SO-PMD statistics at a given wavelength gave nonstochastic PMD distributions with time.

1. Introduction

The polarization mode dispersion (PMD) in deployed fibres is known to evolve in a stochastic pattern due to unpredictable extrinsic perturbations (i.e., environmental changes, vibrations, and human interactions) with time and nonuniform intrinsic perturbations (i.e., core asymmetry and internal stress) experienced along the fibre length. The unpredictable variation of extrinsic and intrinsic perturbations with time and fibre length makes PMD statistics stochastic about some average value, either with wavelength or with time. This means that the PMD of optical systems with time and wavelength is unpredictable; therefore, one must resort to statistical analysis. The statistical property of PMD that attracted the initial interest was the mean first-order PMD (FO-PMD) [1, 2]. Thus, all PMD measurement techniques currently in use in the telecommunication industry require an averaging procedure in order to determine the overall PMD of a fibre link [2, 3].

Most, if not all, of the work done has been focused mainly on FO- and second-order PMD (SO-PMD) statistics, which is likely due to the FO- and SO-PMD vectors being known to be statistically dependent on each other [4, 5]. However, Phua and Haus [6] concluded that FO-PMD can be more accurately characterised than SO-PMD.

Understanding the nature and characteristics of PMD is a key step towards the construction of effective PMD emulators and compensation techniques. The statistical characterisation of PMD includes the probability densities of FO- and SO-PMD, the scaling of the PMD phenomena with changes in the mean FO-PMD, various correlation functions, and characteristics associated with the accuracy of PMD measurements [3]. Efforts have been done also in developing single-end measurement techniques to measure the mean DGD by using polarization sensitive reflectometric techniques [7]. The probability densities for both FO- and SO-PMD in most situations have asymptotic tails extending to unacceptable large impairments best known as outage probability events. All statistical properties hold under the conditions $L \gg L_C$, and L tends to infinity, where L is the fiber length and L_C is the polarization correlation length. While the former condition is usually well verified in all practical conditions, the latter is more critical since the link length is always finite and limited; hence, asymptotic tails are impossible to measure in real conditions.

2. The FO-PMD Statistics

The FO-PMD vector comprises of three vector components which have the independent Gaussian distributions with zero mean and identical variance [2, 8]. This means generating three independent Gaussian random variables and taking their root square sum (RSS) results in a Maxwellian distributed variable. Through implementing the PSP model, the probability density function (PDF) of FO-PMD has been proven to be Maxwellian. The SOPs represented on the Poincaré sphere denote PSP time evolution as a Brownian motion [9].

The probability density function of the FO-PMD in long fibres has been proven to be Maxwellian over time and wavelength [2, 10, 11], whilst its vector components show a Gaussian distribution [12, 13]. The probability density of the FO-PMD was the first PMD density to draw attention [14]. Field measurements have proved the relevancy of the FO-PMD PDF for a very large number of fibre sections, random mode coupling under certain conditions. This has led researchers to design and simulate PMD emulators which reproduce FO-PMD statistics approximating the Maxwellian distribution [10, 15–17]. However, Elbers et al. [18] argues using Monte-Carlo simulations that FO-PMD statistics approximate better to the Rayleigh distribution than the Maxwellian distribution, even though they possessed the same mean value.

Mathematical proof by Gisin and Pellaux [19] showed that for an ideal fibre with infinite random mode coupling and no polarization dependent loss (PDL), the mean FO-PMD at one wavelength measured over a sufficiently long period of time will provide the same result as the mean FO-PMD at a fixed time measured over a sufficiently large wavelength range. Studies, however, have shown that not all fibre FO-PMD values approximate to the idealised Maxwellian distribution [20, 21].

The Maxwellian PDF of the FO-PMD, τ [9, 22] is given by

$$\mathrm{PDF}_{\tau} = \frac{8}{\pi^2 \langle\tau\rangle \left(2\tau_i/\langle\tau\rangle\right)^2} \exp\frac{\left(2\tau_i/\langle\tau\rangle\right)^2}{\pi} \qquad (1)$$

$$\tau_i \geq 0, \quad i = 1, 2, 3, \ldots.$$

Using the Maxwellian PDF, the probability of τ exceeding a particular value can be found using:

$$P(\tau \geq X) = 1 - \int_0^X p(\tau)\, d\tau. \qquad (2)$$

The Rayleigh PDF of the FO-PMD is given by [18]

$$\mathrm{PDF}_{\tau} = \frac{\langle\tau\rangle}{\alpha^2} \exp\left(\frac{\langle\tau\rangle^2}{2\alpha^2}\right), \qquad (3)$$

where

$$\alpha^2 = \frac{8N}{3\pi^3\tau_i}. \qquad (4)$$

Elbers et al. [18] made some confusion which was later rectified by Galtarossa and Palmieri [23]. Galtarossa and Palmieri [23] proved that the FO-PMD (or DGD) is Maxwellian, while the PDF of pulse broadening is Rayleigh distributed. The Rayleigh and the Maxwellian distributions are fitted on FO-PMD measurements and compared in Figure 1.

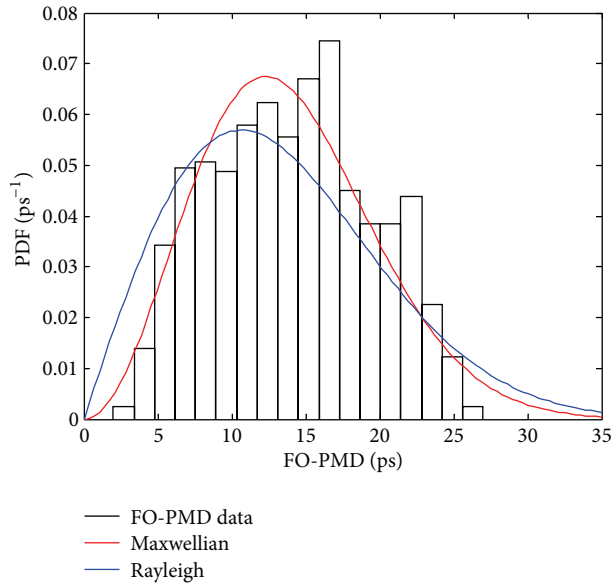

Figure 1: Comparison of the Maxwellian and the Rayleigh distribution fits on the FO-PMD statistics of a 28 km ITU-T G.652 deployed buried fibre link at the Telkom South Africa Sidwell exchange in Port Elizabeth.

The FO-PMD statistics obtained from the field and PMD emulators when the random mode coupling is large approach the Maxwellian distribution best as compared to the Rayleigh distribution, for example, see Figure 1. Therefore this makes the Maxwellian distribution the only used theoretical PDF fit on PMD measurement in this study.

3. The SO-PMD Statistics

Among all higher orders, SO-PMD has drawn significant attention; this is evident through the vast amount of the literature on it [9, 24–27]. SO-PMD is caused by random birefringence changes over the fibre length. The SO-PMD statistics are described by a probability density function first proposed by Foschini et al. [26]. For more information on the statistics of SO-PMD components, namely, PCD and PSP depolarization, the reader is referred to [28–30].

The PDF of the magnitude of the SO-PMD vector $|\vec{\tau}_\omega|$ is [26]

$$\mathrm{PDF}_{|\vec{\tau}_\omega|} = \left(\frac{32|\vec{\tau}_\omega|_i}{\pi\langle\tau\rangle^4}\right) \tanh\left(\frac{4|\vec{\tau}_\omega|_i}{\pi\langle\tau\rangle^2}\right) \mathrm{sech}\left(\frac{4|\vec{\tau}_\omega|_i}{\pi\langle\tau\rangle^2}\right), \quad |\vec{\tau}_\omega|_i \geq 0, \qquad (5)$$

where i is equal to 1, 2, 3, ….

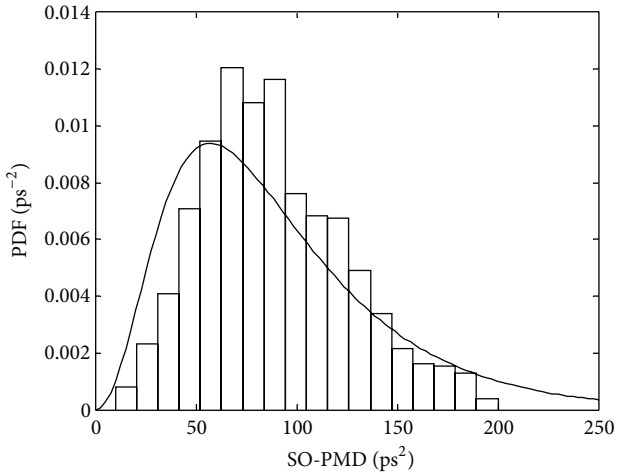

FIGURE 2: The statistical distribution of SO-PMD for a 42 km deployed buried fibre in Port Elizabeth owned by Telkom South Africa. The solid line is the theoretical PDF fit proposed by [26].

The SO-PMD statistics in this study have been compared to the theoretical distribution by [26]. Figure 2 illustrates how the SO-PMD statistics of a 42 km deployed fibre link are close to the SO-PMD theoretical fit. The SO-PMD statistics of the fibre are evidence of the presence of numerous mode coupling sites, random mode coupled, along the fibre length.

4. JME for PMD Measurement

The three input SOPs, as referred above, generate a 2×2 matrix at each wavelength or frequency. In the absence of PDL, the Jones matrix of the nth birefringent section of a fibre link or emulator can be expressed as [31]:

$$T_n = \begin{pmatrix} \cos\theta_n & -\sin\theta_n \\ \sin\theta_n & \cos\theta_n \end{pmatrix} \times \begin{bmatrix} \exp\left(i\frac{\Delta\omega\tau_n}{2}\right) & 0 \\ 0 & \exp\left(-i\frac{\Delta\omega\tau_n}{2}\right) \end{bmatrix} \times \begin{pmatrix} \cos\theta_n & \sin\theta_n \\ -\sin\theta_n & \cos\theta_n \end{pmatrix}, \tag{6}$$

where θ_n is the orientation of the fast axis of the nth section with respect to a fixed axis (say, x-axis), $\Delta\omega = \omega - \omega_o$ is the angular frequency difference with respect to the central frequency ω_o, and τ_n is the FO-PMD (or DGD) of the nth section. The angle θ_n lies between 0° and 360°, and for random mode coupling θ_n is assumed to be uniformly random distributed between this range.

The frequency dependent Jones transfer matrix for the entire fibre link or emulator $T(\omega)$ is a product over T_n for all the N fibre sections:

$$T(\omega) = \prod_{n=1}^{N} \left(\begin{pmatrix} \cos\theta_n & -\sin\theta_n \\ \sin\theta_n & \cos\theta_n \end{pmatrix} \times \begin{bmatrix} \exp\left(i\frac{\Delta\omega\tau_n}{2}\right) & 0 \\ 0 & \exp\left(-i\frac{\Delta\omega\tau_n}{2}\right) \end{bmatrix} \times \begin{pmatrix} \cos\theta_n & \sin\theta_n \\ -\sin\theta_n & \cos\theta_n \end{pmatrix} \right). \tag{7}$$

By measuring the transfer matrix $T(\omega)$ of an entire optical medium, it is possible to determine the total FO-PMD and the PSPs using the standard JME. Heffner [32] showed that the FO-PMD at the angular frequency midway between two closely spaced angular frequencies, ω_1 and ω_2, is given by

$$\tau_{\text{tot}} = \left| \frac{\arg(\rho_1/\rho_2)}{\Delta\omega} \right| = \left| \frac{\arg(\rho_1/\rho_2)}{\omega_2 - \omega_1} \right|, \tag{8}$$

where ρ_1 and ρ_2 are the eigenvalues of the matrix product $T(\omega_2)T^{-1}(\omega_1)$ and arg() is the argument function. The fast and slow PSPs of the fibre are given by the two eigenvectors of $T(\omega_2)T^{-1}(\omega_1)$. Poole and Wagner [33] obtained an expression for the corresponding output PSP for each random concatenated section. When the PSPs are converted to their corresponding stokes representation, the PMD vector in stokes space is as given in (9)

$$\vec{\tau}(\omega) = |\vec{\tau}| \cdot \vec{q} = \Delta\tau \cdot \vec{q}. \tag{9}$$

5. The Generalized Interferometry Technique (GINTY: FTB-5500b)

The generalized interferometric technique (GINTY) developed by EXFO has a modified setup and incorporates different analysis of the interferograms from the one used by TINTY. The main key modification is that GINTY, unlike TINTY, is designed with an algorithm meant to remove the effect of the central autocorrelation peak (ACP), leaving only the cross-correlation peaks (CCPs) used to calculate the FO-PMD value. The ACP contains no FO-PMD information and is known to affect the accuracy of the FO-PMD measurement in TINTY. GINTY removes all the assumptions made when using TINTY for determining FO-PMD [34]. In this section, we highlight how GINTY operates with the support of mathematical equations.

Figure 3 shows an FO-PMD measurement setup, comprising of GINTY. The setup consists of a polarized broadband source, fibre under test (FUT), the Michelson interferometer, polarization beam splitters (PBS), analysers, and the two detectors. The additional polarization beam

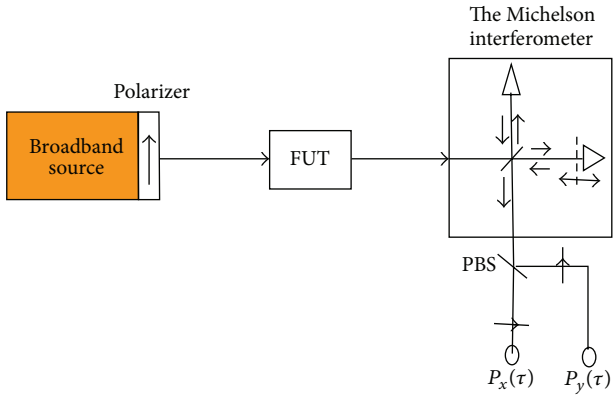

Figure 3: Schematic setup of GINTY.

splitter (PBS) splits the beam and directs it to two detectors for analysis. This setup is used to measure the FO-PMD of a mode coupled fibre resulting in an interferogram with interference fringes. The root mean square (rms) FO-PMD value is then determined from the Gaussian curve fit to the interferogram. The FO-PMD is the distance from the centre of the central peak to the centre of the satellite peak.

Considering general mathematics:

$$\begin{aligned} &\text{Detector 1 : Intensity} = I_1^2 + I_2^2 + 2I_1I_2\cos\theta, \\ &\text{Detector 2 : Intensity} = I_1^2 + I_2^2 - 2I_1I_2\cos\theta, \end{aligned} \tag{10}$$

where I_1^2 is the autocorrelation (AC) from the first arm of the interferometer, I_2^2 is the AC from the second arm of the interferometer, and I_1I_2 is the cross-correlation (CC). GINTY utilises only the CC for accurate FO-PMD measurements.

The autocorrelation and cross-correlation envelopes for a single input/output (I/O) SOP pair are

$$\begin{aligned} \text{AC} : E_o(\tau) &= \left|\widetilde{P}_x(\tau) + \widetilde{P}_y(\tau)\right| \\ &\equiv \text{Detector 1} + \text{Detector 2} = 2\left(I_1^2 - I_2^2\right), \\ \text{CC} : E_x(\tau) &= \left|\widetilde{P}_x(\tau) - \widetilde{P}_y(\tau)\right| \\ &\equiv \text{Detector 1} - \text{Detector 2} = 2\left(2I_1I_2\cos\theta\right), \end{aligned} \tag{11}$$

where $\widetilde{P}_x(\tau)$ and $\widetilde{P}_y(\tau)$ represent the respective raw interferograms observed along the two orthogonal analyser axes.

The exact mathematical analysis gives measured FO-PMD as [34]

$$\text{measured FO-PMD} = \sqrt{\frac{3}{2\left(\sigma_x^2 - \sigma_o^2\right)}}, \tag{12}$$

where σ_x is the root mean square (rms) width of the mean square (MS) CC envelope and σ_o is the rms width of the MS AC envelope. Both MS envelopes are obtained simultaneously but separately without interfering as shown by (11).

GINTY is not sensitive to the source shape spectrum and interferogram shape. The only condition to be satisfied for (12) to apply is that the FUT should exhibit linearity, be stable (although difficult to attain during experiments), and should have zero polarization-dependent loss (PDL). GINTY has an averaging window and remains mathematically exact. Subtraction of the offset, as in (12), eliminates the systematic bias induced by a narrow or ill shaped spectrum, thereby allowing measurements through a network with EDFAs and optical components. In principle, FO-PMD = 0 can be measured when $\sigma_x = \sigma_o$ (12).

6. Results and Discussion

6.1. PMD Measurements. First-order PMD and second-order PMD measurements presented in this section were obtained from ITU-T G.652 28.4 km buried fibres and 14.2 km aerial fibres. These fibres are deployed in South Africa in the city of Port Elizabeth and are owned by Telkom South Africa. All the buried fibre links, each made from looping two 14.2 km fibre links using a single mode patchchord to allow end-to-end access, are secured in a single cable. Buried fibre PMD measurements carried out using the JME method were conducted over the 1520 to 1570 nm wavelength range at an optimal resolution of 0.3 nm to avoid noisy spectra. Aerial fibre PMD measurements were carried out using GINTY since it is not sensitive to fibre movement compared to JME which will introduce measurement errors. The reader should take note that GINTY can also be used for buried fibre measurements. The output SOP of light from an Agilent 8164A laser source was monitored using the A1000 polarization analyser. Single mode fibre (SMF) patchcords with negligible PMD were used to connect the fibre links under test and measurement devices. In this section, firstly, FO-PMD measurements obtained using the JME will be used to determine whether the buried fibre links under test can accommodate high transmission bit rates (≥2.5 Gb/s). Secondly, PMD measurements acquired over wavelength and time will be statistically analysed. In the following section, the focus will be on SOP monitoring with time.

The histogram in Figure 4 shows the mean PMD values obtained when two 14.2 km buried fibre links were looped. The maximum tolerable amount of FO-PMD when transmitting at 2.5 Gb/s is 40 ps, 10 Gb/s is 10 ps, and 40 Gb/s is 2.5 ps. This, therefore, means Telkom South Africa can transmit at 2.5 Gb/s over all the tested fibres without major impediments from PMD. However, an increase in the transmission speed to 10 Gb/s makes fibre links 69-70, 73–75, 75-76, and 78–80 inappropriate for data transmission due to signal impairments. A further increase in transmission speed to 40 Gb/s is not practically feasible for all the fibre links due to all the fibre links having FO-PMD values above 2.5 ps, the maximum tolerable value. Thus, to transmit at high speeds (≥10 Gb/s), Telkom South Africa should replace these fibre links or high birefringent (HiBi) sections along the fibre length

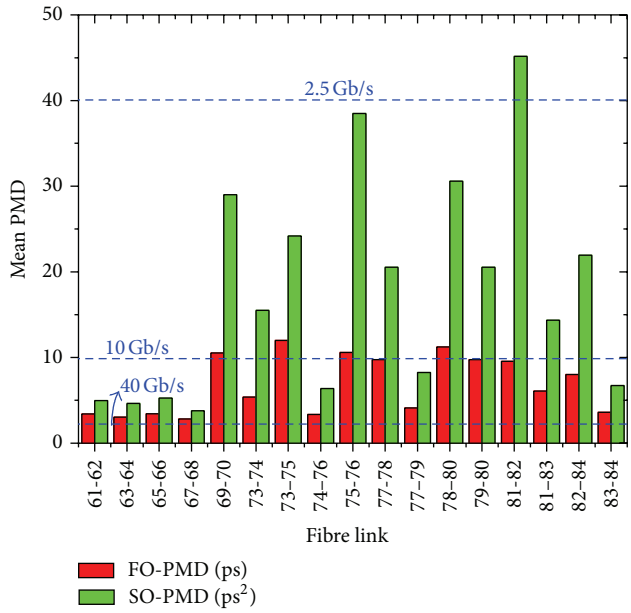

Figure 4: FO- and SO-PMD measurements from 28.4 km ITU-T G.652 buried fibre links. At each transmission bit-rate (2.5 Gb/s, 10 Gb/s and 40 Gb/s), the maximum tolerable amount of FO-PMD corresponds to 10% of the bit period for 1 dB penalty [35].

with those having low PMD. PMD can also be mitigated by the application of PMD compensators. In the next subsection, focus will be on the statistics of PMD with wavelength and time in buried and aerial optical fibres.

6.2. PMD Variation with Wavelength and Time in Buried Fibres. In this subsection, we characterize deployed buried optical fibre links for both FO- and SO-PMD using the JME. The reader should take note that buried fibres are secured in ducts and installed underground. Firstly, PMD variations with wavelength will be analyzed followed by an analysis into their variation with time. The results shown in this subsection are from only some of the buried fibre links, though all fibre links given in Figure 4 were analyzed.

We redrew some parts in Figures 6(a) and 6(b). The results were found to be stochastic in nature and so were their SO-PMD components, namely, PCD and PSP-depolarization. Figure 5 shows the statistical distribution of FO- and SO-PMD obtained from fibre Link 61-62 and link 81-82. These two highlighted links in general represent the PMD statistical behaviour obtained from all the tested fibre links. Figures 5(a′) and 5(b′) provide information (not shown) showing that PSP-depolarization is the dominant SO-PMD contributor compared to PCD. This agrees with findings by Foschini et al. [26], where 8/9 is the expected ratio of PSP-depolarization to SO-PMD. The PSP-depolarization-to-SO-PMD ratio obtained from link 61-62 deviates slightly by 3.4% from the expected value and that of link 81-82 deviates by 9.7% (Figure 5). 1Figures 5(b) and 5(b′) show that the FO-PMD or DGD statistical distribution of link 81-82 approaches the theoretical Maxwellian distribution and that of the SO-PMD approaches the theoretical distribution proposed by Foschini et al. [26]. The PMD distribution from link 61-62 (see Figures 5(a) and 5(a′)) does not approach the theoretical distributions to the same extent. This is likely due to limited random mode coupling that does not promote the significant variation of the FO-PMD and PSPs with wavelength. The former comes from the assumption used by [8] to relate FO-PMD statistics to the Maxwellian distribution. The assumption states that FO-PMD follows a Maxwellian distribution when there is infinite random mode coupling. By comparing the histograms of FO-PMD data obtained from all the fibre links, it can be deduced that the magnitude of the FO-PMD is independent of whether the FO-PMD statistics approach the Maxwellian distribution or not. This means the key factor is sufficient random mode coupling.

SO-PMD measurements show that links with high SO-PMD (Figure 5(b′)) approach the theoretical distribution. This is due to the presence of high random mode coupling which promotes the increased variation of the FO-PMD and PSPs with wavelength. The FO-PMD variation with wavelength is equivalent to PCD and that of PSPs with wavelength is equivalent to PSP-depolarization. Limited mode coupling results in low SO-PMD (Figure 5(a′)). Take note that there is not always a linear relationship between FO- and SO-PMD as was observed with the tested fibres. The PMD emulator designs show that in some cases, FO-PMD and SO-PMD are inversely proportional, FO-PMD is fixed but SO-PMD varies and vice versa, and negligible SO-PMD can yield varying FO-PMD [21].

In order to monitor PMD (both FO- and SO-PMD) with time over a fibre link, the computer was programmed to continuously sample PMD versus wavelength statistics at 1 minute intervals over a 98-hour period. Measurements were taken from fibre link 63-64, the results of which are presented in Figure 6. It can be deduced from Figure 6 that the PMD changes with time at a fixed wavelength were gradual and had limited variations. These gradual and limited PMD variations are probably due to limited temperature changes on the fibre links. This results in limited changes in fibre birefringence and mode coupling. These findings agree with the work by [36] who found limited PMD changes with time. However, slight temperature changes or movement that may occur on the looped SMF patchcord can affect the SOP of light and the coupling angle between the two 14.2 km fibre links. This coupling angle can affect the total PMD of the link per wavelength. This SMF patchcord can be referred to as a Hinge. To monitor the behaviour of the Hinge with time, a Hinge model has been developed. A Hinge site is a discrete location along a fibre link which is exposed to environmental perturbations usually where buried fibres lead to optical devices along the network system. The variation of PMD with wavelength at a fixed time in this study was stochastic. This is due to the presence of random mode coupled along the length of the fibre link.

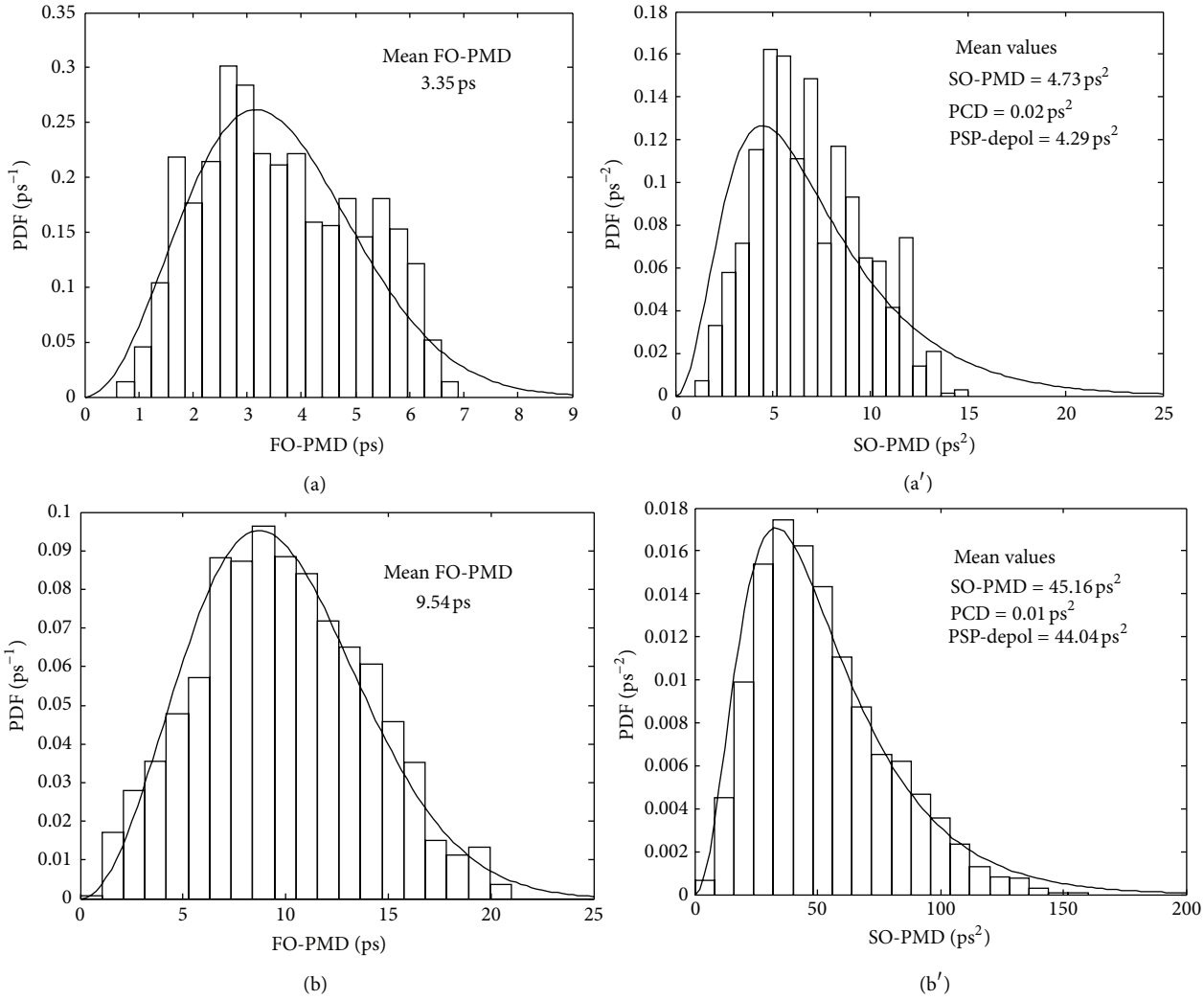

Figure 5: The FO-PMD statistical distribution for (a) link 61-62 and (b) link 81-82 and the accompanying SO-PMD statistical distribution for (a′) link 61-62 and (b′) link 81-82. The solid line mapped to the FO-PMD histogram is the theoretical Maxwellian distribution and that mapped to the SO-PMD histogram is the theoretical distribution proposed by Foschini et al. [26].

Each wavelength has independent PMD vectors (FO- and SO-PMD vectors). Therefore, regions where the SO-PMD magnitude increases (Figure 6 (b′)), for example, between 40–63 hrs at 1526.32 nm and 63–80 hrs at 1555.50 nm, indicate a reduction in the angle separating these two vectors (one of link 63 and the other of link 64). In this case, the SMF patchcord region, which can be referred to as the Hinge, determines the angle between the two vectors. When there is a decreasing trend in the SO-PMD (e.g., between 63–83 hrs at 1526.32 nm and 40–63 hrs at 1555.50 nm), the reverse is true. A large separation angle (≈180°) between two SO-PMD vectors of almost similar magnitude will give a decreasing resultant SO-PMD approaching zero. A smaller vector separation angle (≈0°) will give a resultant SO-PMD vector which is almost equivalent to the sum of the two vectors. A similar argument as above could be used to describe the trend observed in the FO-PMD with time in Figure 6(a′). If one of the vectors dominates the other, the resultant vector will be close to the dominant vector even if the separation angle between these vectors ranges from 0 to 180°.

Figures 6(a′) and 6(b′) show a distinctive behaviour of the two PMD phenomena (FO- and SO-PMD); they do not necessarily follow the same trend or direction at particular wavelengths with time. This difference likely emanates from their definitions; definition FO-PMD is considered wavelength-independent and SO-PMD is considered frequency dependent. The unevenness in SO-PMD changes with time as in Figure 6(b′) is most likely due to the measurement error of the JME. The SO-PMD vector at any particular wavelength is also affected by rotating vectors at adjacent neighboring wavelengths. The gradual and limited FO- and SO-PMD between the 1-minute time over the 98-hour period results in nonstochastic FO- and SO-PMD distributions, which do not approach the PMD theoretical distributions. A

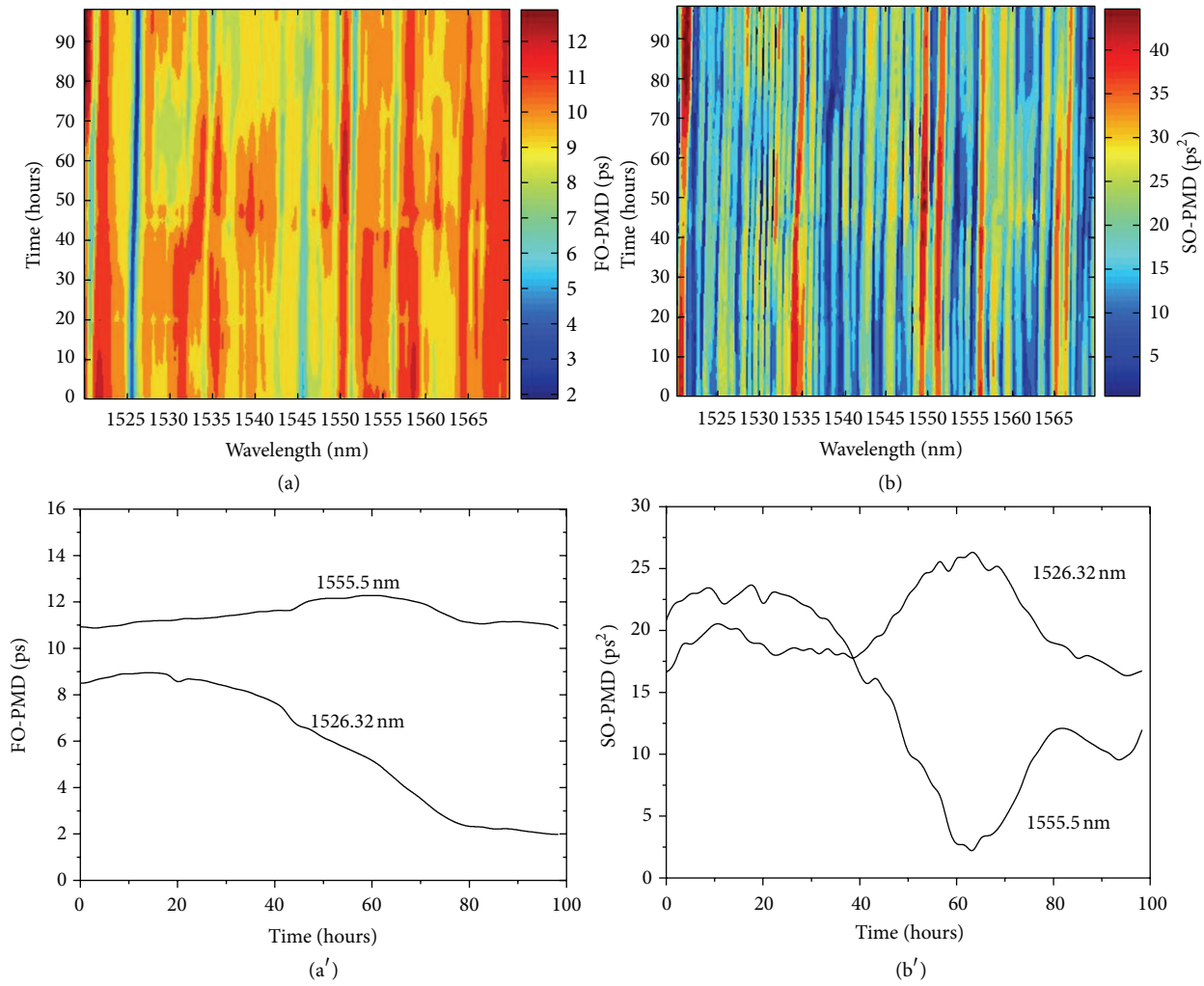

Figure 6: (a) FO-PMD and (b) SO-PMD versus wavelength and time density maps for a coupled fibre link. This coupled link is a result of coupling links 63 and 64. An illustration of (a′) FO-PMD and (b′) SO-PMD behaviour with time at the 1526.32 and 1555.50 nm wavelengths.

nonstochastic PMD distribution will still be maintained over a long period of time if these external perturbations remain limited or vary gradually.

7. Conclusion

Telkom South Africa has to replace optical fibre links or the high birefringent sections along the optical fibre network with those having low PMD values for it to transmit at high speeds of ≥10 Gb/s.

In a period of 98 hours, the PMD variation with wavelength was found to be directional and limited. That is, the PMD changes at a given wavelength were found to be minimal and were due to mode coupling in the optical fibre link.

Acknowledgments

This work was supported in part by Telkom SA Ltds., Ingoma Communication Services, Dartcom, the African Laser Centre, the National Research Foundation, the National Laser Centre, and THRIP.

References

[1] D. Andresciani, F. Curti, F. Matera, and B. Diano, "Measurement of the group-delay difference between the principal states of polarization on a low-birefringence terrestrial fiber cable," *Optics Letters*, vol. 12, pp. 844–846, 1987.

[2] J. P. Gordon and H. Kogelnik, "PMD fundamentals: polarization mode dispersion in optical fibers," *Proceedings of the National Academy of Sciences of the United States of America*, vol. 97, no. 9, pp. 4541–4550, 2000.

[3] N. Gisin, B. Gisin, J. P. Von Der Weid, and R. Passy, "How accurately can one measure a statistical quantity like polarization-mode dispersion?" *IEEE Photonics Technology Letters*, vol. 8, no. 12, pp. 1671–1673, 1996.

[4] J. N. Damask, *Polarization Optics in Telecommunication*, Springer, New York, NY, USA, 1st edition, 2005.

[5] A. Galtarossa and C. R. Menyuk, Eds., *Optical Fiber Communication Reports*, Springer, New York, NY, USA, 2005.

[6] P. B. Phua and H. A. Haus, "Variable second-order PMD module without first-order PMD," *Journal of Lightwave Technology*, vol. 20, no. 11, pp. 1951–1956, 2002.

[7] F. Corsi, A. Galtarossa, L. Palmieri, M. Schiano, and T. Tambosso, "Continuous-wave backreflection measurement of polarization mode dispersion," *IEEE Photonics Technology Letters*, vol. 11, no. 4, pp. 451–453, 1999.

[8] G. J. Foschini and C. D. Poole, "Statistical theory of polarization dispersion in single mode fibers," *Journal of Lightwave Technology*, vol. 9, no. 11, pp. 1439–1456, 1991.

[9] F. Curti, B. Daino, G. De Marchis, and F. Matera, "Statistical treatment of the evolution of the principal states of polarization in single-mode fibers," *Journal of Lightwave Technology*, vol. 8, no. 8, pp. 1162–1166, 1990.

[10] A. O. Dal Forno, A. Paradisi, R. Passy, and J. P. von der Weid, "Experimental and theoretical modeling of polarization-mode dispersion in single-mode fibers," *IEEE Photonics Technology Letters*, vol. 12, no. 3, pp. 296–298, 2000.

[11] M. Karlsson, J. Brentel, and P. A. Andrekson, "Long-term measurement of PMD and polarization drift in installed fibers," *Journal of Lightwave Technology*, vol. 18, no. 7, pp. 941–951, 2000.

[12] C. De Angelis, A. Galtarossa, G. Gianello, F. Matera, and M. Schiano, "Time evolution of polarization mode dispersion in long terrestrial links," *Journal of Lightwave Technology*, vol. 10, no. 5, pp. 552–555, 1992.

[13] M. Brodsky, P. Magill, and N. J. Frigo, "Polarization-mode dispersion of installed recent vintage fiber as a parametric function of temperature," *IEEE Photonics Technology Letters*, vol. 16, no. 1, pp. 209–211, 2004.

[14] C. D. Poole, J. H. Winters, and J. A. Nagel, "Dynamical equation for polarization dispersion," *Optics Letters*, vol. 16, pp. 372–374, 1991.

[15] Y. Lizé, P. Lavoie, N. Godbout, S. Lacroix, R. Kashyap, and L. Palmer, "Novel first and second order polarization mode dispersion emulator," in *Proceedings of the Optical Fiber Communication Conference (OFC/NFOEC '05)*, pp. 563–565, March 2005, paper OThT1.

[16] R. Khosravani Jr., I. T. Lima, P. Ebrahimi, E. Ibragimov, A. E. Willner, and C. R. Menyuk, "Time and frequency domain characteristics of polarization-mode dispersion emulators," *IEEE Photonics Technology Letters*, vol. 13, no. 2, pp. 127–129, 2001.

[17] L. S. Yan, M. C. Hauers, C. Yeh et al., "High-speed, stable and repeatable PMD emulator with tunable statistics," in *Proceedings of the Optical Fiber Communications Conference (OFC '03)*, vol. 1, pp. 6–7, 2003, paper MF6.

[18] J. P. Elbers, C. Glingener, M. Düser, and E. Voges, "Modelling of polarisation mode dispersion in singlemode fibres," *Electronics Letters*, vol. 33, no. 22, pp. 1894–1895, 1997.

[19] N. Gisin and J. P. Pellaux, "Polarization mode dispersion: time versus frequency domains," *Optics Communications*, vol. 89, no. 2–4, pp. 316–323, 1992.

[20] H. Sunnerud, C. Xie, M. Karlsson, R. Samuelsson, and P. A. Andrekson, "A comparison between different PMD compensation techniques," *Journal of Lightwave Technology*, vol. 20, no. 3, pp. 368–378, 2002.

[21] V. Musara, L. Wu, A. Leitch, S. Younsi, and M. Zghal, "Statistical characterization of first-order and second-order polarization mode dispersion in a deployed buried optical fibre cable," in *Proceedings of IEEE Africon*, pp. 1–6, September 2009.

[22] N. Gisin, R. Passy, J. C. Bishoff, and B. Perny, "Experimental investigations of the statistical properties of polarization mode dispersion in single mode fibers," *IEEE Photonics Technology Letters*, vol. 5, no. 7, pp. 819–821, 1993.

[23] A. Galtarossa and L. Palmieri, "Relationship between pulse broadening due to polarisation mode dispersion and differential group delay in long singlemode fibres," *Electronics Letters*, vol. 34, no. 5, pp. 492–493, 1998.

[24] L. E. Nelson, R. M. Jopson, H. Kogelnik, and G. J. Foschini, "Measurement of depolarization and scaling associated with second-order polarization mode dispersion in optical fibers," *IEEE Photonics Technology Letters*, vol. 11, no. 12, pp. 1614–1616, 1999.

[25] V. Musara, L. Wu, G. Pelaelo, and A. W. R. Leitch, "Polarization mode dispersion emulation using polarization maintaining fibers: fixed root-mean-square differential group delay but varying second-order polarization mode dispersion," *Review of Scientific Instruments*, vol. 80, no. 5, Article ID 053113, 5 pages, 2009.

[26] G. J. Foschini, R. M. Jopson, L. E. Nelson, and H. Kogelnik, "Statistics of PMD-induced chromatic fiber dispersion," *Journal of Lightwave Technology*, vol. 17, no. 9, pp. 1560–1565, 1999.

[27] Z. Zalevsky and V. Eckhouse, "Polarization-mode dispersion manipulation using periodic polarization modulation," *Journal of Optics A*, vol. 6, no. 9, pp. 862–868, 2004.

[28] G. J. Foschini, L. E. Nelson, R. M. Jopson, and H. Kogelnik, "Probability densities of second-order polarization mode dispersion including polarization dependent chromatic fiber dispersion," *IEEE Photonics Technology Letters*, vol. 12, no. 3, pp. 293–295, 2000.

[29] E. Forestieri, "A fast and accurate method for evaluating joint second-order PMD statistics," *Journal of Lightwave Technology*, vol. 21, no. 11, pp. 2942–2952, 2003.

[30] G. J. Foschini, L. E. Nelson, R. M. Jopson, and H. Kogelnik, "Statistics of second-order PMD depolarization," *Journal of Lightwave Technology*, vol. 19, no. 12, pp. 1882–1886, 2001.

[31] D. Gupta, A. Kumar, and K. Thyagarajan, "Effect of second-order polarization mode dispersion on the performance of polarization mode dispersion emulators," *Optical Engineering*, vol. 46, no. 8, Article ID 085006, 2007.

[32] B. L. Heffner, "Automated measurement of polarization mode dispersion using Jones matrix eigenanalysis," *IEEE Photonics Technology Letters*, vol. 4, no. 9, pp. 1066–1069, 1992.

[33] C. D. Poole and R. E. Wagner, "Phenomenological approach to polarization dispersion in long single-mode fibres," *Electronics Letters*, vol. 22, no. 19, pp. 1029–1030, 1986.

[34] N. Cyr, "Polarization-mode dispersion measurement: generalization of the interferometric method to any coupling regime," *Journal of Lightwave Technology*, vol. 22, no. 3, pp. 794–805, 2004.

[35] C. D. Poole and J. Nagel, "Polarization effects in lightwave systems," in *Optical Fiber Telecommunications*, I. P. Kaminow and T. Koch, Eds., Academic, San Diego, Calif, USA, 1997.

[36] H. Kogelnik, P. J. Winzer, L. E. Nelson, R. M. Jopson, M. Boroditsky, and M. Brodsky, "First-order PMD outage for the hinge model," *IEEE Photonics Technology Letters*, vol. 17, no. 6, pp. 1208–2499, 2005.